


Analysis of changes in air pollution and its relationship with social isolation due to the COVID-19 pandemic in Brazilian Northeast

*Laízy de Santana Azevedo*¹ 

*Ana Lúcia Bezerra Candeias*² 

*João Rodrigues Tavares Júnior*³ 

Keywords:

Satellite Images
Coronavirus
Nitrogen Dioxide
Aerosol Optical Depth

Abstract

In March 2020, the World Health Organization declared the Covid-19 a pandemic. It was considered that social isolation measures adopted to slow the spread of the virus, could have reduced the level of pollutants such as nitrogen dioxide (NO₂) and AOD (Aerosol Optical Depth). Therefore, this research identified changes in atmospheric air pollution in Northeast Brazil through MODIS Terra / Aqua AOD and Sentinel 5P-TROPOMI images to investigate changes in AOD and NO₂, respectively, during the first half of 2020 compared to the same period in 2019. The result revealed that NO₂ in almost the entire Territory decreased in the second two months of 2020 (-4.49%), which corresponds to the beginning of social blocks. The third bimester showed an increase of 2.26%. Regarding AOD, despite the slowdowns in social interaction, there was no significant drop. Pollutant levels were also checked in urban, industrial areas and around water reservoirs and the results showed similarity between the analyzes carried out for the Northeast and these areas.

INTRODUCTION

At the end of 2019, an epidemic event began in China. The outbreak of a virus, called the new coronavirus (SARS-CoV-2), was declared a pandemic in March by the World Health Organization (WHO, 2020). In this context, social isolation measures were implemented to reduce this virus contagion. These measures have led to reductions in aerosols and air pollutants in various parts of the world.

Studies carried out by NASA (2020) have shown that air pollution has decreased, mainly in China, due to social distancing measures established to delay this virus's spread. Authors such as Ranjan *et al.*, (2020) observed that social blockages caused pollution reductions in urban areas of India. However, in mining areas, pollution increased. In Brazil, researchers have also carried out similar studies focusing on the Southeast region of the country (DANTAS *et al.*, 2020; BRANDÃO, 2020)

Understanding how air pollution is affected by extreme disruptions in social relationships due to Covid-19 can provide important information regarding air pollutant mission control. According to the United Nations – UN (2019), the world population is expected to increase by about 2 billion people in the next 30 years. This accelerated growth is one of the main consequences of air pollution increase (KAPLAN AND AVDAN, 2020). Population growth combined with exposure to air pollutants generate negative impacts on the environment and human health quality (HOU *et al.*, 2019). Therefore, the study of air pollutants is essential since they negatively affect the population.

Satellite image usage to detect air quality changes has been employed to observe several pollutants in the stratosphere and troposphere. Among them, we can highlight Nitrogen Dioxide (NO₂) and aerosols.

NO is one of the main components of urban air pollution, generated mainly by anthropic actions (BECHLE *et al.*, 2013). It is a polluting gas with a strong smell and brown color concentrated close to polluting sources, giving a dark tone to the environment with higher concentration rates. High concentrations of this gas can cause respiratory and lung problems and lead to photochemical smog and acid rain formation.

The AOD (Aerosol Optical Depth) is a dimensionless physical parameter that indicates how much aerosols attenuate the radiation beam as it propagates through a specific layer of the atmosphere containing

aerosols. They can be defined as solid or liquid particles suspended in the atmosphere from both natural and anthropogenic sources, including mineral dust from the soil, soot, and gases from volcanic eruptions, biogenic forest material, biomass burning, among others (PRADO; COELHO, 2017). They affect atmospheric stability, precipitation, the hydrological cycle, vegetation cover, and its growth, in addition to increased respiratory problems in humans (LAL *et al.*, 2020)

Conventionally, air quality is monitored from ground stations. However, despite accurately indicating air pollutant concentration levels, these measurements on the ground present limited monitoring due to the high cost and sparse spatial coverage. In this sense, remote sensing has advantages, providing information about air pollution in large areas quickly and efficiently (SOUZA *et al.*, 2017).

Given this, this research verified air pollutants levels changes in the Northeast region of Brazil as a whole, also analyzing some areas considered potential sources of pollutant emissions and areas suffering negative impacts from air pollution. In addition, we also sought to study the relationship between air pollutants and social isolation caused by the Covid-19 pandemic. The study was carried out by processing satellite images from TROPOMI Sentinel – 5P and MODIS AOD throughout the first half of 2019 and 2020. The study was conducted using the data processing platform of Google Earth Engine (GEE), making the images available to be processed in the cloud.

Sentinel's NO₂ product – 5P (Precursor) is part of the Copernicus global monitoring program dedicated to atmospheric monitoring (ESA, 2020). The mission consists of a satellite with the instrument Tropospheric Monitoring Instrument (TROPOMI), whose main objective is to perform atmospheric measurements with a high spatiotemporal resolution for air quality, ozone, and ultraviolet radiation studies, along with climate monitoring and forecasting. The satellite was launched in October 2017 in Russia and has reported a resolution of 0.01 degrees (ESA, 2020).

The AOD MODIS product globally monitors the optical thickness of the aerosol over oceans and continents (NASA, 2020). Aerosol optical depth (AOD) is a measure of columnar atmospheric aerosol content. The MODIS (Moderate Resolution Imaging Spectroradiometer) is an instrument aboard the Terra and Aqua satellites. After years in operation, a new Multiangle Implementation of Atmospheric Correction (MAIAC) algorithm

was developed for MODIS providing daily AOD data with a spatial 1 km resolution (CHUDNOVSK *et al.*, 2014).

MATERIALS AND METHODS

Study area

The study area comprises the Northeast of Brazil, one of the country's five regions (Figure 1). This region was chosen due to the lack of studies related to air pollution in this area. According to the Instituto de Energia e Meio Ambiente (IEMA-2018), only nine of the twenty-seven Brazilian states monitor air quality. The vast majority of them are concentrated in the south and southeast regions of the country.

As this region is quite extensive in territorial dimension, in addition to a comprehensive analysis in its entirety, some strategic regions called "test areas" were also chosen to verify changes in air pollution in more detail during the pandemic.

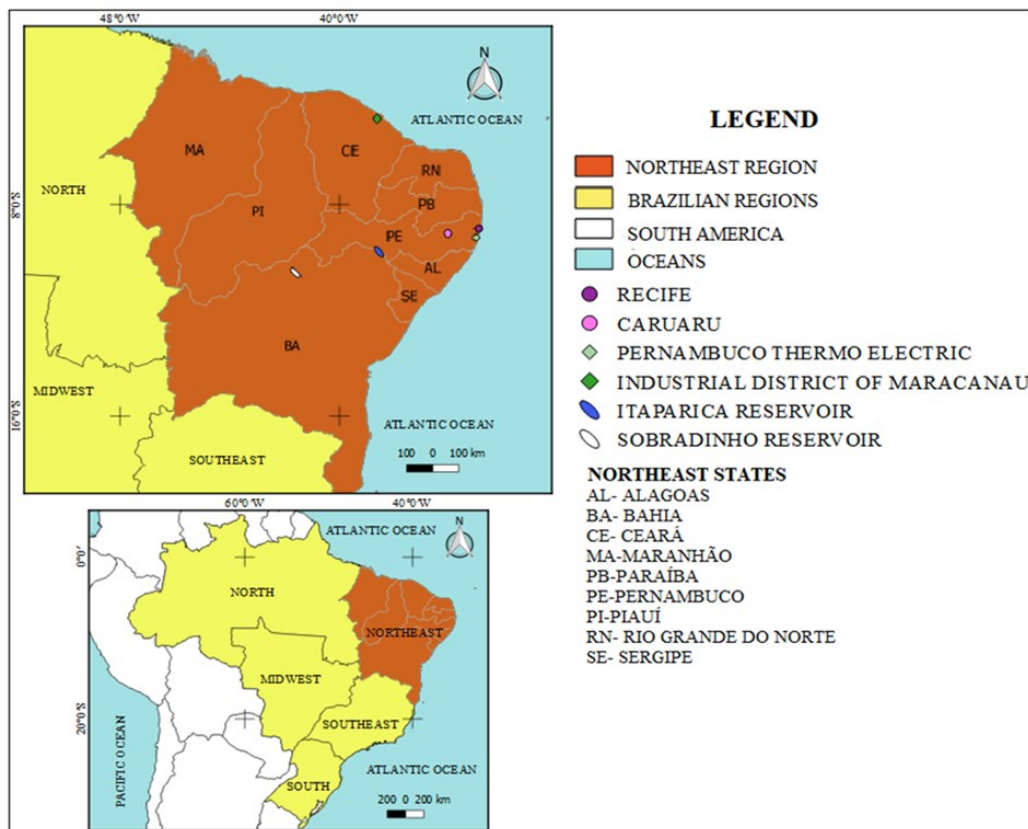
Areas considered potential sources of pollutant emission and areas suffering negative impacts from air pollution were chosen. The chosen regions comprise urban areas, industrial

areas, and water reservoirs' surroundings. The urban areas correspond to the cities of Recife and Caruaru-PE. The areas of industrial activities were the thermoelectric power plant of Pernambuco and the industrial district of Maracanaú CE and the surroundings of the water reservoirs of Sobradinho and Itaparica – BA and PE, respectively.

The urban areas were chosen considering intense vehicular circulation, areas of industrial activities because of these activities' nature, they are considered potential pollution sources, and the surroundings of the reservoirs to check the pollutant levels close to important water sources. For the analysis of the results, the delimitation of the two cities was made according to their municipal limits. For industrial areas and water reservoirs, a buffer of 10 km was considered, starting from the centroid and its borders, respectively.

In all states in the Northeast region, the recommendation of social distancing began in mid-March 2020. In addition, some regions adopted even more intense restriction periods, as was the case in Recife – PE on May 16th to 31st, 2020 (PERNAMBUCO 2020), São Luís - MA on April 3rd to May 20th, 2020 (MARANHÃO, 2020) and Fortaleza-CE on May 8th to 20th, 2020 (FORTALEZA, 2020).

Figure 1 – Map of the study area localization.



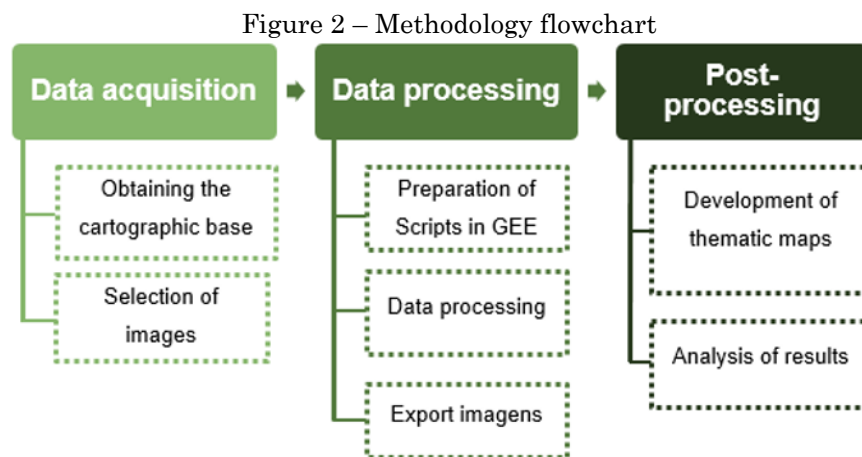
Source: The authors.

MATERIALS E METHODS

For this article development, the following materials and technological resources were used: Images from the Terra/Aqua satellite instrument MODIS-AOD and Sentinel Images - 5 Precursor instrument TROPOMI – NRTI NO₂, files in shapefile format provided by the Instituto Brasileiro de Geografia e Estatística (IBGE) and

the Agência Nacional de Águas e Saneamento Básico (ANA), Google Earth Engine Platform, Social isolation data provided by the company in-loco and the Ministério Público de Pernambuco (MPPE), QuantumGIS Software version 2.18.16, Software Excel 2016 and hp core i5 notebook Windows 10 operating system

The methodology applied in the development of this research can be seen in the flowchart in the Figure below



Source: The authors.

Initially, the study area was delimited in the scripts' preparation in the GEE for data acquisition. The cartographic base in the shapefile format used for this purpose was obtained from the IBGE website (2020). Shapefile files for the test areas were also obtained from IBGE and ANA (2020). For the NO₂-related studies, Sentinel-5P TROPOMI images were used, while for the AOD studies, terra and Aqua/MODIS images were used. The images were taken from collections made available by the GEE, which owns partner products and makes them available for free for research, education, and non-profit use.

Regarding Data Processing, in the script preparation in Java language in the GEE, it was also defined, through filters, the study period from January to June 2019 and 2020 for NO₂ and AOD. MODIS AOD products have historical images from 2000 to the present time. The Sentinel 5P NO₂ product, on the other hand, provides data from July 2018, so the year 2020 was compared only with 2019 to verify whether there were significant changes in the levels of pollutants in 2020. To compile the data to be analyzed in the results, the images were grouped into bimesters: the 1st bimester - January and February, the 2nd bimester - March and April, and the 3rd bimester - May and June.

In addition to the filters for delimiting the

study area and period, an average filter was also applied to calculate the average NO₂ and AOD variation per two months. The AOD data are dimensionless, whereas the NO₂ data are expressed in $\mu\text{mol}/\text{m}^2$, with the minimum estimated value being $-600 \mu\text{mol}/\text{m}^2$ and the maximum $96001444.34 \mu\text{mol}/\text{m}^2$.

The images obtained within each collection were selected by observing the incidence of clouds over the study area during the analyzed period. MODIS and Sentinel data have a band indicating the probability of cloud presence in a given pixel ranging from 0 (no clouds) to 1 (covered with clouds). Therefore, pixels were checked, and the average cloud coverage showed values up to 0.4 in all images to avoid misleading results.

Furthermore, to guarantee the quality of the images, the data comes with a quality assurance band called 'qa_value' indicating the pixel quality on a scale from 0 (bad) to 1 (good), derived from several factors such as the presence of clouds, surface albedo, snow/ice, signal saturation, and acquisition geometry. Before being inserted into the GEE, the data is filtered to remove low-quality pixels with 'qa_value' < 0.75 (ALI et al., 2021).

Data were processed in the cloud within the GHG platform. Despite the study area being quite extensive, the computational capacity of the GEE processed the data in a few minutes displaying the results on the screen. These results were then

exported, also programmatically, to Google Drive. This step was necessary because the GHG only generates visible results, not allowing thematic maps layout within the platform.

In the Post-Processing stage, after obtaining the results within the GHG platform and having these data in Google Drive, the images were downloaded and imported into the QuantumGIS software (QGIS) to prepare thematic maps.

Then, the images were classified, and the maps were obtained. It was decided to present in the same layout the data for every two months of the year 2020 and 2019 to facilitate the comparison of changes in pollutant levels through visual analysis. Based on the processed bimonthly images, the temporal variation of the concentration of the two pollutants for each state was further explored. From the thematic maps, standardized anomalies were calculated to obtain statistical data on changes from one year to another. These data provided a clearer idea of how much pollutant levels diverged between the two study periods. Anomalies were calculated using equation 1.

$$anomaly = \frac{x - \bar{x}}{\sigma \bar{x}} \tag{1}$$

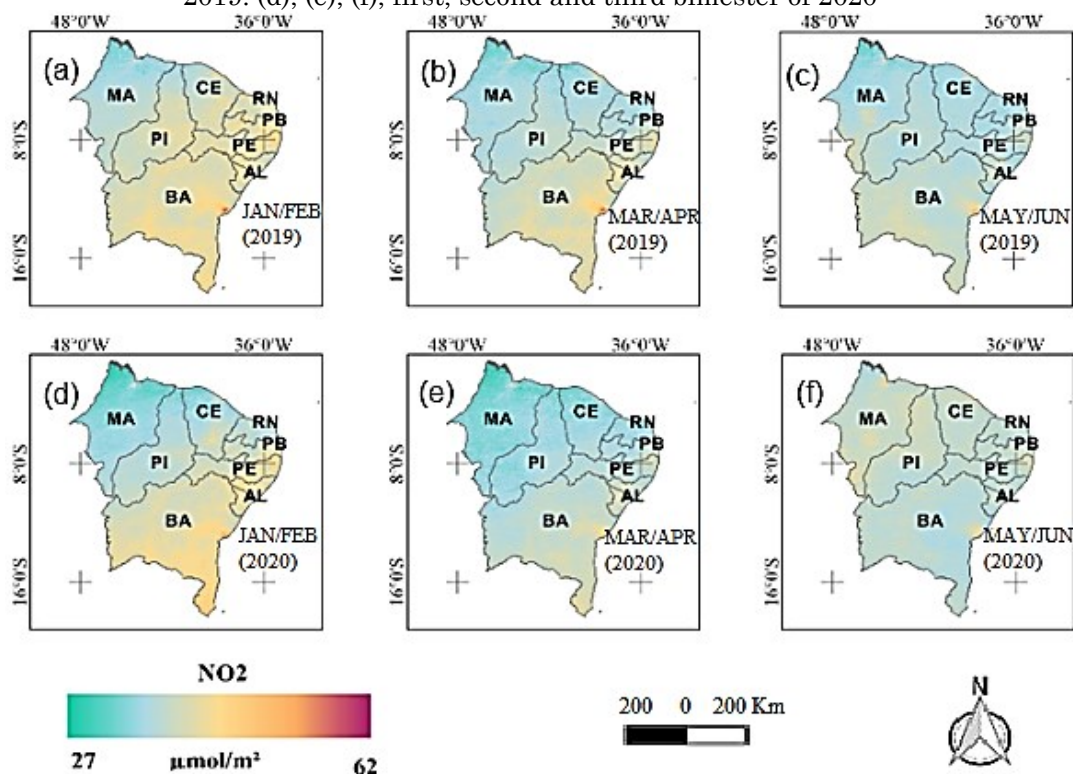
where x is the bi-monthly average NO₂/AOD for 2020 in μmol/m² for the NO₂, and dimensionless for the AOD, and \bar{x} is the bi-monthly average NO₂/AOD for 2019, and $\sigma \bar{x}$ is the standard

deviation of these data. These calculations were performed using the QGIS raster calculator. Anomalies were calculated for each northeastern state and the test areas. The numerical data obtained from the images were used in the Excel software to elaborate anomaly graphs. Finally, these graphs were visually associated with social isolation indexes due to Covid-19 provided by the company in loco and the Ministério Público de Pernambuco (MPPE, 2020).

RESULTS AND DISCUSSION

Initially, the results for NO₂ will be presented, in which the maps in Figure 3 show the average distribution of this pollutant in the northeastern territory. Visually, it can be identified that most states, except Maranhão and Piauí in the third bimester, have a higher average for 2019 than 2020. Also, there is a significant reduction in NO₂ levels in all states during the second bimester of 2020. The range of classes was defined by analyzing each image's minimum and maximum values, and the same cutoff point was adopted so that the data could be compared. The lowest value observed was 27 and the highest 62, representing the NO₂ concentration in μmol/m².

Figure 3- Map of changes in NO₂ levels. (a), (b) and (c), the first, second, and third bimester of 2019. (d), (e), (f), first, second and third bimester of 2020



Source: The authors.

The numerical results of the image above can be seen in Table 1. It shows the NO₂ average concentration for the three bimesters of 2019 and 2020 and the percentage variation. It

appears that the most significant decrease was for the second two months (-4.49%), while for the third two months there was an increase of 2.26%.

Table 1- Mean NO₂ variation (μmol/m²) per bimester

Bimester	Year		Percentage variation (%)
	2019	2020	
1° bimester	40.263	38.870	-3.460
2° bimester	38.321	36.601	-4.490
3° bimester	37.541	38.391	+2.260

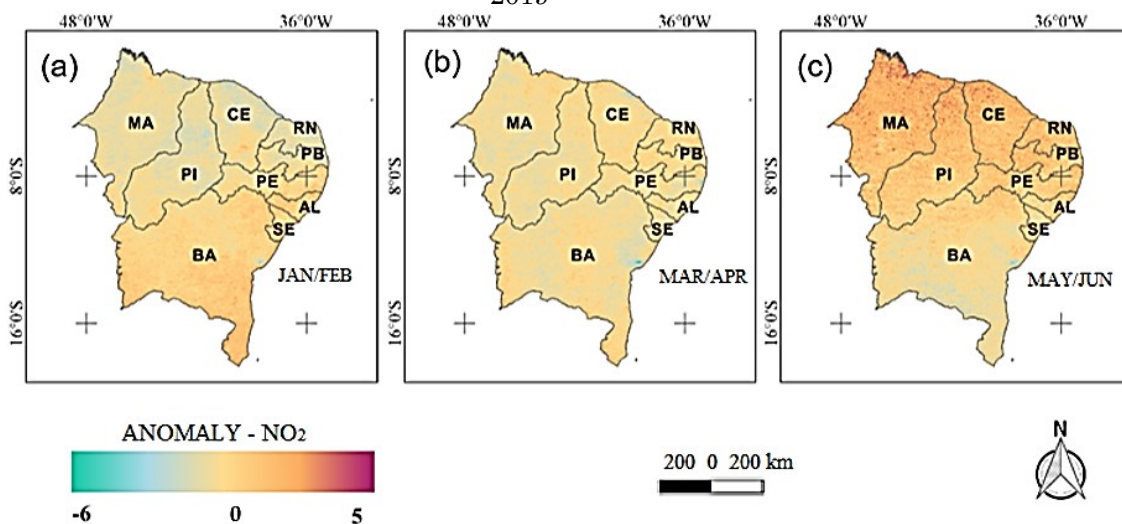
Source: The authors.

For better visualization of the changes that occurred in the analyzed period, the standardized anomaly of NO₂ of each two months was estimated through Equation 1. Also, a map of the average spatial variation of this gas during the year 2020 was generated

compared to the average for the year 2019 (Figure 4).

On this map, negative values (green to yellow color) point to a decrease in the level of this pollutant, while positive values (orange to wine color) show an increase in NO₂

Figure 4- NO₂ anomalies. (a), (b) and (c) first, second and third bimester of 2020 compared to 2019

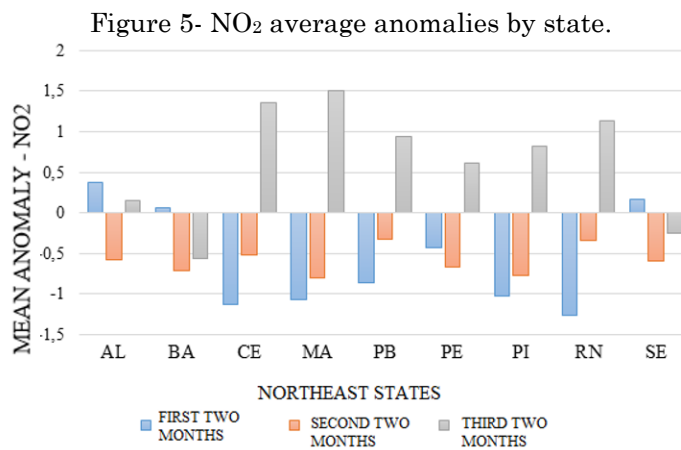


Source: The authors.

From Figure 4, it can be seen, in general, a significant NO₂ reduction, especially in the second two months, which corresponding to March and April. Yellow color is predominant, indicating that the anomaly results are negative for most of the territory. In this same period, it is worth highlighting the regions close to the capitals of Bahia (BA) and Pernambuco (PE) shown on the map in blue, showing that the values are even lower in these regions there was a reduction in the pollutant concentration. In the first semester, it is also noticeable that the anomaly values are negative in a large part of the Northeast, emphasizing the Bahia region, which is an exception. It presents pixels classified closer to orange color, indicating positive anomalies and

slight increases in this gas concentration. In the third bimester, it is possible to visualize an increase in NO₂ compared to the previous two months due to pixels classified in red wine color.

For these results to be better analyzed, a numerical analysis of the NO₂ average anomalies by the state was performed, as shown in Figure 5. Through the bar diagram graph, the maximum and minimum NO₂ anomalies of +1.50 can be seen, and -1.25 for the third bimester of the state in Maranhão (MA) and the first two months in the Rio Grande do Norte (RN), respectively. All states showed negative anomalies for the second bimester and positive anomalies in the third bimester, except for Bahia and Sergipe (SE), which in the third bimester showed a downward trend.



Source: The authors.

Still, regarding the generated anomalies interpretation, a pollutant concentration classification was made. Subsequently, the areas occupied by each class were calculated, verifying the percentage that each one occupied in the

Northeast region. The results can be seen in Table 2, where it is noted that the largest area for all bimesters corresponding to classes around 0, indicating that there were no significant changes between the studied years in most of the territory.

Table 2- Area of NO₂ anomalies by class in Square Kilometers

CLASS	AREA OF NO ₂ ANOMALIES (Square Kilometers)					
	1° BIMESTER	ÁREA (%)	2° BIMESTER	ÁREA (%)	3° BIMESTER	ÁREA (%)
-6 a -4	0.000	0.000	36000.000	0.020	44040.000	0.030
-4 a -2	2608000.000	1.650	1244000.000	0.790	1005000.000	0.640
-2 a 0	116600000.000	73.800	54890000.000	34.750	143900000.000	91.140
0 a 2	38770000.000	24.540	86190000.000	54.560	12990000.000	8.230
2 a 5	23330.000	0.010	15640000.000	9.900	0.000	0.000

Source: The authors.

These results can be associated with the social isolation indexes resulting from COVID-19 provided by the company in loco since the pollutants' emission is strictly related to human activities. Several researchers have sought to relate the lockdown effects on air pollution in

various world regions (Berman and Ebisu, 2020; Ranjan et al., 2020). Table 3 shows the social isolation indexes by state, exhibiting the population percentage complying with the recommendation to stay at home in each analyzed bimester.

Table 3- Social isolation indexes in the Northeastern states.

STATES	1° bimester	2° bimester	3° bimester
ALAGOAS	30.480%	38.310%	38.980%
BAHIA	29.050%	34.600%	38.970%
CEARÁ	29.470%	34.850%	38.840%
MARANHÃO	29.220%	34.730%	38.810%
PARAÍBA	29.220%	34.640%	39.750%
PERNAMBUCO	30.130%	39.190%	40.160%
PIAUI	30.050%	39.100%	40.120%
RIO GRANDE DO NORTE	30.310%	38.860%	40.090%
SERGIPE	28.520%	37.500%	38.370%

Source: The authors (2020).

It is possible to notice that in all Northeastern States, the highest rates of social isolation point to the second and third bimesters. According to Baldasano (2020), this period corresponds to the rapid pandemic growth period in several countries, resulting in the need to isolate the population as the main way to reduce the disease spread.

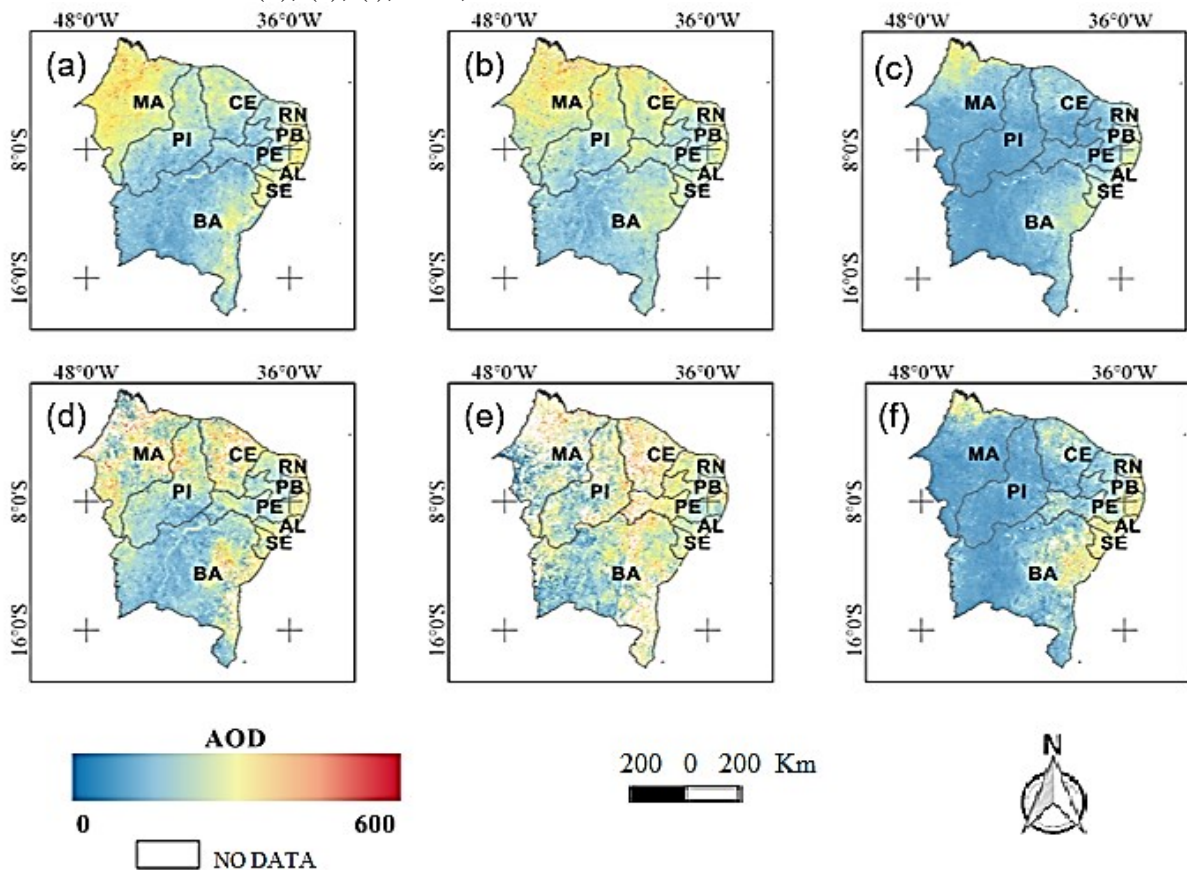
As a result, there was a restriction on the vehicle circulation in many municipalities and a stoppage of several industries and services: stores, hotels, and restaurants leaving only essential activities in various locations. In some cities, there were even periods of even more intense restrictions, such as Recife - PE (PERNAMBUCO, 2020), São Luís - MA (MARANHÃO, 2020), and Fortaleza-CE (FORTALEZA, 2020).

Many researchers have pointed out that there is evidence that the change in the concentration

of pollutants is, at least in part, related to the economic slowdown after the coronavirus outbreak (BALDASANO, 2020; BERMAN AND EBISU, 2020; NASA, 2020). As of the third bimester, many activities began to be resumed, leading to a reduction in isolation rates and, consequently, to an increase in pollution. This post-isolation growth was also observed by researchers in various regions of the world, mainly in China, considered the disease's epicenter (NASA, 2020; REUTERS, 2020).

Figure 6 shows the distribution of AOD in the northeastern territory. The range of classes was defined by analyzing each image's minimum and maximum values, and the same cutoff point was adopted so that the data could be compared. The lowest value observed was 0, and the highest was 679, which represents the concentration of AOD. Visually, it is noted that most northeastern states have a higher average for 2020 than for 2019.

Figure 6- Map of changes in AOD levels. (a), (b) and (c) first, second and third bimester of 2019. (d), (e), (f), first, second and third bimester of 2020.



Source: The authors.

The numerical results of the image above can be seen in Table 4. It shows the mean AOD concentration for the three bimesters of 2019 and 2020 and the variation in percentage. It can

be seen that the greatest decrease was for the third bimester (-6.20%), and the smallest was for the second bimester, in which there was an increase of 11.39%.

Table 4- Average variation in AOD per bimester.

Bimester	YEAR		Percentage variation (%)
	2019	2020	
1° bimester	208.000	208.720	+0.350
2° bimester	219.840	244.890	+11.390
3° bimester	128.050	120.120	-6.200

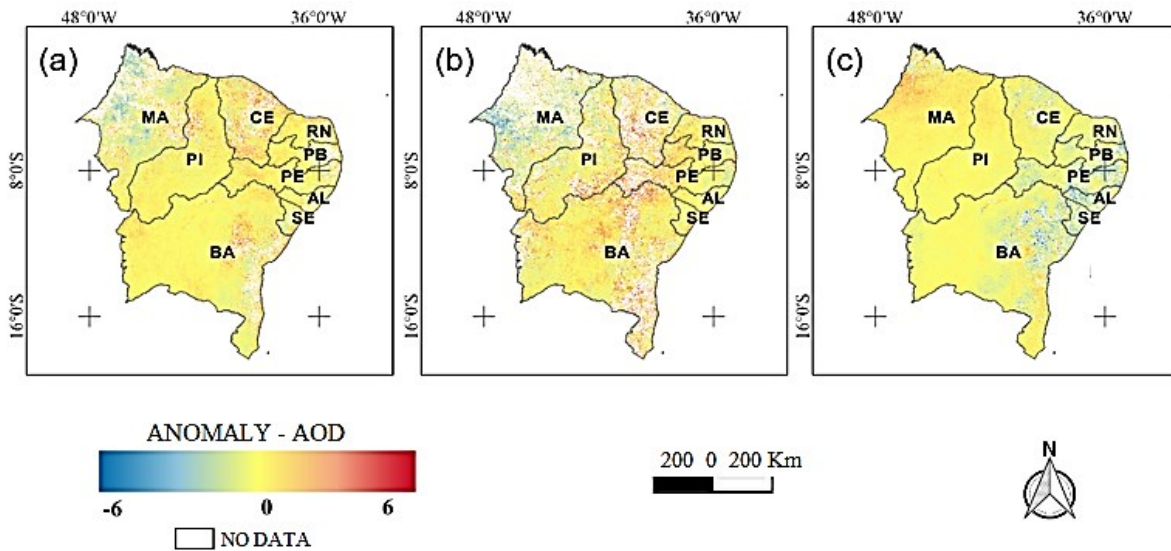
Source: The authors.

To better understand changes distribution in AOD levels in the northeastern territory, the standardized AOD anomaly for each bimester period was also estimated using Equation 1.

The AOD anomaly map can be seen in Figure

7, where negative values (from blue to yellow color) point to a decrease in the level of this pollutant, while positive values (from yellow to red color) show an increase in AOD levels.

Figure 7- AOD anomalies. (a), (b) and (c) first, second and third bimester of 2020 compared to 2019.



Source: The authors.

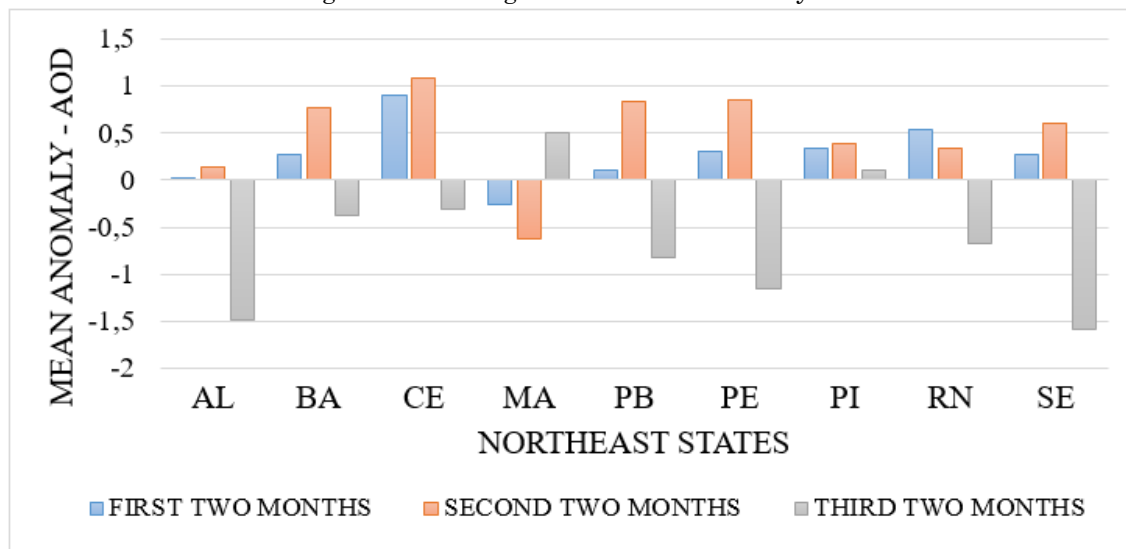
Note that there were no significant changes in most of the study area between 2019 and 2020, with anomalies around zero (yellow color). However, it is possible to visualize changes in AOD levels in some specific regions. During the third bimester, negative anomalies (blue color) were found mainly in the coastal region. While in the first two bimesters, positive anomalies are noted in some stretches in the central region. These results were verified due to the presence of the classes in red color indicating positive anomalies, around 6, and an increase in the AOD levels.

Mainly in the second bimester, there are some regions with missing data, represented in white color. MODIS AOD is retrieved using the dark target algorithm. Data availability in some regions is affected by the presence of shiny surfaces. According to Levy et al. (2010), the

AOD recovery of MODIS becomes challenging in regions with high surface reflectance. However, these data are widely accepted in academia because several validation studies have proven that about 72% of ODA recoveries are within expected uncertainty levels (REMER et al., 2005; LEVY et al., 2010).

For these results to be better analyzed, a numerical analysis of the average AOD anomalies by the state was performed, as shown in Figure 8. From the bar diagram, the maximum and minimum AOD anomalies of +1.07 and - 1.50 for the second bimester in the state of Ceará and the third bimester in Sergipe, respectively. There are negative anomalies in almost all states for the third two months, except for Maranhão (MA) and Piauí (PI), and positive anomalies in all states for the first and second two months, except for Maranhão.

Figure 8 – Averages of AOD anomalies by state.



Source: The authors.

Despite the possible slowdowns in social life, the results showed that the isolation indexes were not enough to significantly decrease the AOD levels in the first two bimesters regarding 2019. Authors such as Ranjan et al. (2020) carried out similar studies to those seeking to verify the effects of the blockage caused by Covid-19 on ODA levels in urban and mining regions in India. According to these authors, the reasons for a higher AOD level are unclear, even with the effects of the blocking periods. However, this increase may indicate recent polluting sources in these locations compared to the previous period. In addition, the AOD data of some pixels in the study region were missing, which may cause the AOD level to be lower than the actual values.

Therefore, the results can be justified by the inconsistency in AOD pixels number within the administrative limits of the Northeast during the periods corresponding to 2019 and 2020. The total AOD pixels count within the administrative limits of the states was not the same in all cases. Therefore, there may be a slight variation in the AOD anomaly throughout the northeastern territory. Baldasano (2020) also says another

essential factor is that the trucks continued to circulate during the partial blockade, as industrial and construction activities and the food transport and cargo, in general, were maintained. Another hypothesis discussed by several authors is that aerosols are not only emitted into the atmosphere by anthropogenic sources, otherwise being generated through various physical and chemical processes (SEINFELD; PANDIS, 2006).

Still, regarding the generated anomalies interpretation, an AOD concentration classification was also made. Later, the areas occupied by each class were calculated, verifying the percentage that each one occupied concerning the Northeast region. The results can be seen in Table 5. It is noted that the largest area in all bimesters corresponds to classes around 0, indicating no significant changes between the years studied. However, it is noteworthy that in the first and second two months, mainly, the sum of the areas of each class was lower than the actual value due to the absence of AOD data in some parts of the images.

Table 5- AOD anomalies area by class in square kilometers

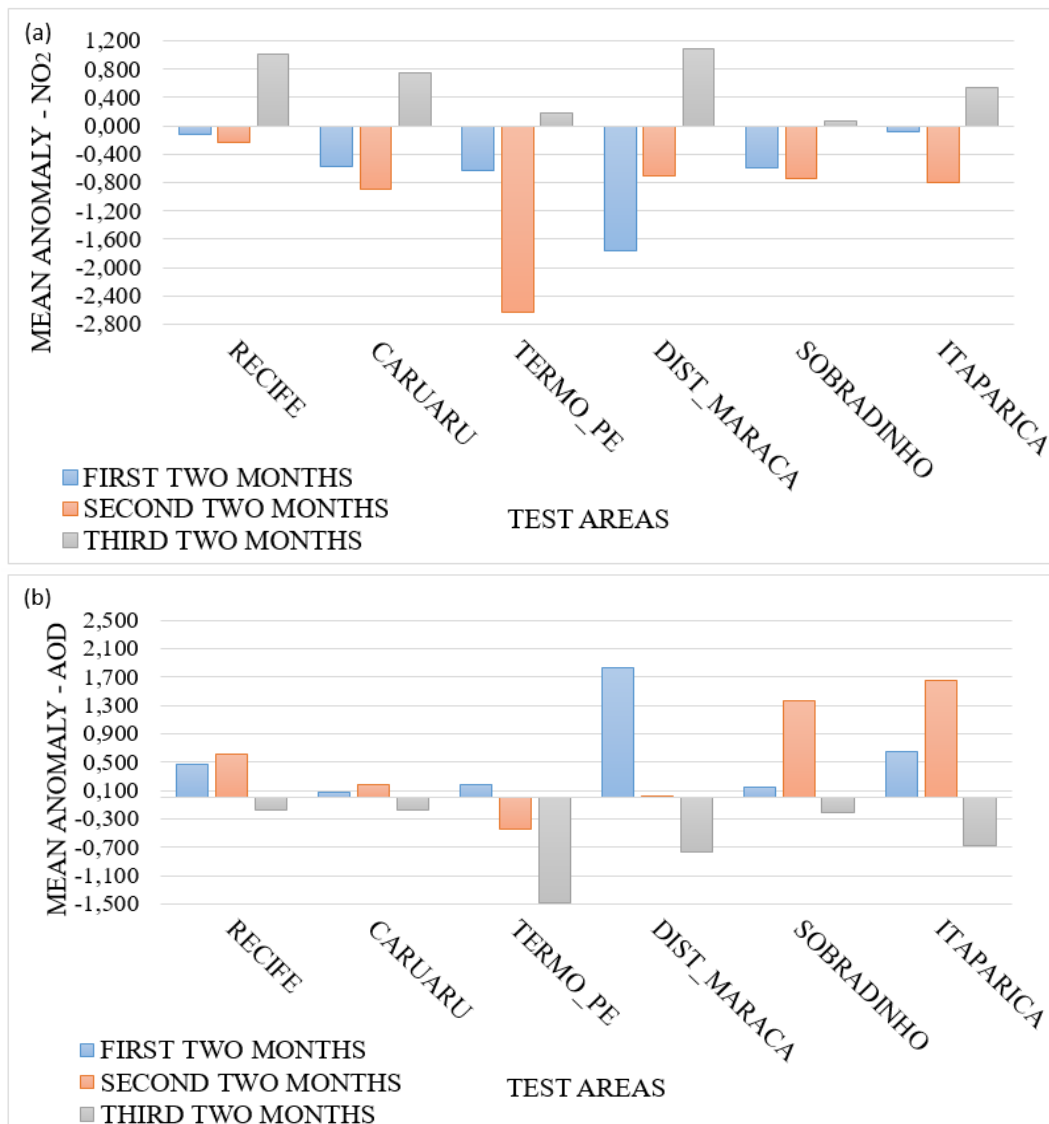
CLASS	AOD ANOMALIES AREA (square kilometers)					
	1º BIMESTER	AREA IN %	2º BIMESTER	AREA IN %	3º BIMESTER	AREA IN %
≤-6 to -3	2293000.000	1.620	2608000.000	2.070	1123000.000	0.070
-3 to 0	62010000.000	43.920	38240000.000	30.370	75740000.000	50.020
0 to 3	71500000.000	50.640	66530000.000	52.830	71400000.000	47.150
3 to 5	5333000.000	3.780	11870000.000	9.430	3870000.000	2.560
5 to ≥6	65760.000	0.050	6675000.000	5.300	307300.000	0.200

Source: The authors.

We also sought to verify changes in NO₂ and AOD pollutants in some strategic areas. Therefore, average anomaly data were clipped for

these areas. This cut was made to allow a more detailed analysis of pollutant variations (Figure 9).

Figure 9 – Averages of NO₂ (a) and AOD (b) anomalies by test areas.



Source: The authors.

It is essential to highlight that in addition to social isolation, other factors also affect the pollutant dispersion in the atmosphere, such as precipitation. Thus, different rainfall regimes may have caused changes in pollutant concentrations in 2019 and 2020 (DANTAS et al., 2020). It is also noteworthy that the AOD permanence time in the atmosphere is longer than that of NO₂. Also, aerosols can be transported to distant regions, unlike NO₂, which is concentrated close to the place of its emission (FILONCHYK et al., 2020).

The results obtained show coherence between the analysis carried out for the whole region and the test areas. However, for NO₂, there is a decrease in the two bimesters, and for AOD, this

decrease only occurs in the third bimesters (Figures 4 and 8).

The Figure 9a analysis shows negative anomalies in all test areas in the first and second two months. On the contrary, the third bimester has positive anomalies in all areas, especially in the Pernambuco and Sobradinho thermoelectric plant, also positive but smaller than in the other areas.

Figure 9b results show positive anomalies for almost all areas in the first and second bimesters, except for the second two months of the Suape thermoelectric plant, which was negative. The third bimester showed negative anomalies in all areas.

Analyzing the cities of Recife and Caruaru, the

decrease observed in the first two bimesters for the NO₂ pollutant can be explained by the isolation rates, where the highest rates were concentrated from March to mid-May for both cities. This phenomenon is due to NO₂ emissions strictly related to anthropogenic actions (CLARK et al., 2018; ALBERS, 1994).

Another critical factor that may have contributed to the reduction of NO₂ levels is that in mid-March, the Pernambuco government issued a decree (Decree No. 48832 of 03/19/2020), considering the country's health authorities recommendation and of the state seeking to reduce the flow of people in collective spaces, to mitigate the dissemination of the coronavirus in Pernambuco.

After this stricter restriction, economic recovery measures were initiated, and insulation rates began to decrease, and consequently, NO₂ levels rose again. This decrease followed by a pollutant level increase was also observed by NASA researchers (2020) in the China region.

Regarding the industrial areas, the NO₂ level behavior was the same as in the other areas. Thus, although there was no total stoppage of industrial activities during the pandemic, there may have been a partial reduction in their functioning due to the employees' number decrease and input purchasing difficulty.

The detailed results for the two cities and industrial areas regarding AOD were similar. Therefore, they can be justified for the same reasons as in the analysis carried out by the state where isolation indexes were not enough to significantly decrease AOD levels in the first two bimesters in 2019.

In Brazil, Dantas et al. (2020) evaluated the social blockade impacts in Rio de Janeiro city regarding carbon monoxide (CO), NO₂, particulate materials, and ozone (O₃). The results showed that the partial population confinement, the reduction of road traffic, and economic activity led to a decrease in low NO₂ levels. This is because heavy vehicles powered by diesel, trucks, and buses contributed 91 and 96% of nitrogen oxides, respectively. During the partial blockage, trucks continued to circulate, as industrial and construction activities were maintained, as well as food transportation and cargo in general. As a result, aerosols were reduced only during the first week of partial blockage.

Brandão (2020) analyzed changes in air quality in São Paulo (SP) and Rio de Janeiro (RJ), combining satellite and terrestrial data. Daily NO₂ and aerosol data were explored for May between 2015-2020. Average decreases of 45% were found for 2020 compared to the 2015-2019 period average. For aerosols, no significant

change was observed for the same period. However, the high number of fires in the Southeast region was highlighted, which may have affected the results.

For Filonchyk et al. (2020), who studied NO₂, CO, and AOD before and during the pandemic in eastern China, the COVID-19 blockade improved air quality in the short term, until coal consumption in power plants and refineries returned to normal levels due to activities resumption. CO and NO₂ showed a significant decrease (20 and 30%, respectively). In contrast, AOD showed high values, and this may have been caused by the much longer residence time of aerosol particles in the atmosphere than a few hours for NO₂. As a result, they can be transported over long distances from where they were generated, unlike NO₂, which is concentrated close to its polluting sources.

Regarding the surroundings of the water reservoirs for both NO₂ and AOD, Silva et al. (2011) state that monitoring becomes a difficult task for managing agencies due to the large size of the reservoirs, and those anthropic actions can help in processes such as eutrophication and water acidification. NO₂, for example, reacts with water present in the air, forming nitric acid (HNO₃), one of the main components of acid rain that causes aquatic environments acidification (CHIUFFA, 2018). Thus, aquatic environments can suffer from chemical contaminants from aerosols and other atmospheric pollutants. The results obtained showed that the pollutant levels in these regions showed behaviors similar to those in urban and industrial areas, showing the need for pollutant monitoring in these areas.

CONCLUSIONS

The current research showed that the level of NO₂ in almost the entire Northeastern Territory was reduced in the second bimester of 2020, with a drop of 4.49%, corresponding to the pandemic rapid growth period and the beginning of the social blockade events triggered by Covid-19. On the other hand, the third bimester, marked by the economic recovery, presented an increase of 2.26%.

The results showed that despite the slowdowns in social life, there was no significant decrease in ODA levels in the first two bimesters of 2020 compared to 2019, each with an increase of 0.35% and 11.39% respectively. One possible justification for this is that the AOD data of some pixels in the study region were absent; therefore, AOD levels may have lowered compared to the actual values. This occurrence is one of the

analysis limitations presented in this work, the non-extraction of values from some AOD pixels for some locations. In this sense, the results could slightly vary if all pixel values were considered. However, based on our results and those of other researchers, it is believed that this study's main conclusions remain valid. For the third bimester, a 6.19% AOD level reduction was observed.

Pollutant level verification in the strategic areas adopted in this research revealed a similarity between the analysis for the whole Northeast region and the test areas. NO₂ levels decreased in the first two bimesters. For AOD, this decrease only occurred in the third bimester. Thus, from the analysis carried out, it is concluded that satellite images can be a good alternative for monitoring air quality compared to terrestrial monitoring stations, as these have limited monitoring due to their high cost and low spatial coverage. In addition, this monitoring is essential to understand the impacts of anthropogenic activities on air pollutant emission.

REFERENCES

- ALBERS, W. M. Indoor air pollution: NO, NO₂, CO, and CO₂. **The journal of allergy and clinical immunology**, v. 94, n. 2, p. 289-295, 1994. [https://doi.org/10.1016/0091-6749\(94\)90088-4](https://doi.org/10.1016/0091-6749(94)90088-4).
- ALI, G. et al. 2021. Environmental impacts of shifts in energy, emissions, and urban heat island during the COVID-19 lockdown across Pakistan. **Journal of Cleaner Production**, v. 291, p. 125806, 2021. <https://doi.org/10.1016/j.jclepro.2021.125806>.
- ANA – AGÊNCIA NACIONAL DE ÁGUAS E SANEAMENTO BÁSICO, 2020. **ANA metadata catalog**. Available: <https://metadados.snirh.gov.br/geonetwork/srv/por/catalog.search#/home>. Access in: 10/07/2020.
- BALDASANO, J. M. COVID-19 lockdown effects on air quality by NO₂ in the cities of Barcelona and Madrid (Spain). **Science of The Total Environment**, v.741, n.1 p. 140353, 2020. <https://doi.org/10.1016/j.scitotenv.2020.140353>.
- BRANDÃO, R. **Atmospheric Pollutant Levels in Southeast Brazil During COVID-19 Lockdown: Combined Satellite and Ground-based Data Analysis**. 2020. Dissertation (Master in Environmental Engineering) – faculty of the Virginia, Polytechnic Institute and State University, Virgínia, 2020. Available: <https://vtechworks.lib.vt.edu/handle/10919/102026>. Access in 05/06/2020.
- BECHLE, M. J.; et al. Remote sensing of exposure to NO₂: satellite versus ground-based measurement in a large urban area. **Atmos. Environ.**, v. 69, p. 345-353, 2013. <https://doi.org/10.1016/j.atmosenv.2012.11.046>.
- BERMAN, J. D.; EBISU, K. Changes in U.S. air pollution during the COVID-19 pandemic. **Science of the total environment**, v. 739, p. 139864, 2020. <https://doi.org/10.1016/j.scitotenv.2020.139864>.
- CHUDNOVSKY, A.; LYAPUSTIN, A.; WANG, Y.; TANG, C.; SCHWARTZ, J.; KOUTRAKIS, P. High resolution aerosol data from MODIS satellite for urban air quality studies. **Central European Journal of Geosciences**, v. 6, n. 1, p. 17-26, 2014. <https://doi.org/10.2478/s13533-012-0145-4>.
- CLARK, L. P.; MILLTE, D. B.; MARSHALL, J. D. National Patterns in Environmental Injustice and Inequality: Outdoor NO₂ Air Pollution in the United States. **PLoS ONE**, v. 9, n. 4, p. 94431, 2018. <https://doi.org/10.1371/journal.pone.0094431>.
- CHIUFFA, V. P. D. **Analysis of the emission and deposition of air pollutants that affect aquatic environments through the operation of a distribution center**. 2018. Dissertation (Master in Civil Engineering) – Faculty of Engineering of Ilha Solteira Campus - UNESP, Paulista State University “Júlio De Mesquita Filho”, Ilha Solteira, 2018. Available: <https://repositorio.unesp.br/bitstream/handle/11449/180145/2-s2.0-85052680129.pdf?sequence=1&isAllowed=y>. Access in: 12/05/2020.
- DANTAS, G. et al. The impact of COVID-19 partial lockdown on the air quality of the city of Rio de Janeiro, Brazil. **Science of the Total Environment**, v. 729, 139085 p., 2020. <https://doi.org/10.1016/j.scitotenv.2020.139085>.
- ESA – Agência Espacial Europeia, 2020. **Sentinel – 5P**. Available at: <https://sentinel.esa.int/web/sentinel/missios/sentinel-5p>. Access in: 11/10/2020.
- FILONCHYK, M.; et al. Impact Assessment of COVID-19 on Variations of SO₂, NO₂, CO and AOD over East China. **Aerosol and air quality research**, v. 20, n. 7, p. 1530-1540, 2020. <https://doi.org/10.4209/aaqr.2020.05.0226>.
- FORTALEZA. DECREE No. 14663 of 05/05/2020. Establishes, in the city of Fortaleza, the Rigid Social Isolation Policy as a measure to confront COVID - 19, and other measures. Available: <https://www.legisweb.com.br/legislacao/?id=394831>. Access in: 11/02/2020.
- GEE- **GOOGLE EARTH ENGINE**. Available: <https://earthengine.google.com/>. Access in:

- 11/06/2020.
- GEE- GOOGLE EARTH ENGINE, 2020. **Sentinel-5P NRTI NO2: Near Real-Time Nitrogen Dioxide**. Available at: https://developers.google.com/earth-engine/datasets/catalog/COPERNICUS_S5P_NRTI_L3_NO2. Access in: 11/09/2020.
- HOU, Y.; WANG, L.; ZHOU, Y.; WANG, S.; LIU, W.; ZHU, J. Analysis of the tropospheric column nitrogen dioxide over China based on satellite observations during 2008–2017. **Atmospheric Pollution Research**, v. 10, n. 2, p. 651-655, 2019. <https://doi.org/10.1016/j.apr.2018.11.003>.
- IBGE – Instituto Brasileiro de Geografia e Estatística, 2020. **Territorial divisions**. Available: <https://www.ibge.gov.br/geociencias/organizacao-do-territorio/malhas-territoriais.html>. Access in: 11/12/2020.
- IBGE – Instituto Brasileiro de Geografia e Estatística, 2016. **agricultural census**. Available: <https://biblioteca.ibge.gov.br/visualizacao/livros/liv61914.pdf>. Access in: 11/12/2020.
- IEEMA- Instituto de Energia e Meio Ambiente, 2018. **National Air Quality Platform**. Available: <http://energiaeambiente.org.br/>. Access in: 10/11/2020.
- INLOCO- **Covid-19 Brazilian Map**, 2020. Available: <https://mapabrasileirodacovid.inloco.com.br/pt/>. Access in: 10/11/2020.
- KAPLAN, G., ADVAN, Z. Y. Space-borne air pollution observation from sentinel-5p tropomi: relationship between pollutants, geographical and demographic data. **International Journal of Engineering and Geosciences (IJEG)**, v. 5, n. 3, p. 130-137, 2020. <https://doi.org/10.26833/ijeg.644089>.
- LAL, P. et al. The dark cloud with a silver lining: Assessing the impact of the SARS COVID-19 pandemic on the global environment. **Science of the total environment**, v. 732, p. 139297, 2020. <https://doi.org/10.1016/j.scitotenv.2020.139297>.
- LEVY, R.C. et al. Global evaluation of the collection 5 MODIS dark-target aerosol products over land. **Atmospheric Chemistry and Physics**, v. 10, p. 10399-10420, 2010. <https://doi.org/10.5194/acp-10-10399-2010>.
- MARANHÃO. DECREE No. 35784 of 05/03/2020. Establishes the preventive and restrictive measures to be applied on the Island of Maranhão (São Luís, São José de Ribamar, Paço do Lumiar and Raposa), pursuant to COVID-19. Available: <https://www.legisweb.com.br/legislacao/?id=394644>. Access in: 11/02/2020.
- MPPE- Ministério Público de Pernambuco. **Social isolation ranking**. 2020. Available at: https://datastudio.google.com/u/0/reporting/1CaZl5DfH_Ohj1wmb7mArBDpdZkna1r9q/page/LSrOB?s=p3vHxnrBoWE. Access in: 11/21/2020.
- MOURA, R. S. T.; LOPES, Y. V. A.; SILVA, G. G. H. Sedimentation of nutrients and particulate matter in a reservoir under the influence of fish farming activities in the semi-arid region of Rio Grande do Norte. **New Chemistry**, v.37, n. 8, p. 1283-1288, 2014. Available: <http://static.sites.s bq.org.br/quimicanova.s bq.org.br/pdf/v37n8a04.pdf>. Access in: 11/13/2020.
- NASA - Administração Nacional do Espaço e da Aeronáutica, 2020. **Airborne Nitrogen Dioxide Plummets Over China**. Available: <https://earthobservatory.nasa.gov/images/146362/airborne-nitrogen-dioxide-plummets-over-china>. Access in: 11/13/2020.
- NASA - Administração Nacional do Espaço e da Aeronáutica, 2020. **Nitrogen Dioxide Levels Rebound in China**. Available: <https://earthobservatory.nasa.gov/images/146741/nitrogen-dioxide-levels-rebound-in-china>. Access in: 11/13/2020.
- OMS – Organização Mundial de Saúde, 2020. **Joint Mission Report Who-China on Coronavirus Disease 2019 (Covid-19)**. Available at: <https://cutt.ly/on20Fbb>. Access in: 11/13/2020.
- OMS - Organização Mundial de Saúde, 2016. **Ambient air pollution: A global assessment of exposure and burden of disease**. Available at: <https://www.who.int/phe/publications/air-pollution-global-assessment>. Access in: 11/13/2020.
- PERNAMBUCO. DECREE No. 48832 of 03/19/2020. Define, in the socioeconomic sphere, additional temporary restrictive measures to face the public health emergency of international importance resulting from the Coronavirus. Available: <https://www.legisweb.com.br/legislacao/?id=390952>. Access in: 11/02/2020.
- PERNAMBUCO. DECREE No. 49017 of 05/11/2020. Provides for the intensification of restrictive measures, of an exceptional and temporary nature, aimed at containing the Covid-19 dissemination curve. Available: <https://www.legisweb.com.br/legislacao/?id=395175>. Access in: 11/02/2020.
- PRADO, N. V.; COELHO, S. M. S. C. 2017. Study of the Temporal Variability of the Optical Depth of the Aerosol Using Remote Sensing Data on the Transition Region between the Amazon Forest and the Cerrado. **Brazilian magazine of meteorology**, v. 32, n. 4, 2017. <https://doi.org/10.1590/0102-7786324012>.
- RANJAN, A. K.; PATRA, A. K.; GORAI, A. K. Effect of lockdown due to SARS COVID-19 on

- aerosol optical depth (AOD) over urban and mining regions in India. **Science of The Total Environment**, v. 745, n. 25, p. 141024, 2020. <https://doi.org/10.1016/j.scitotenv.2020.141024>.
- REMER L.A. et al. The MODIS aerosol algorithm, products, and validation. **Journal of the Atmospheric Sciences**, v. 62, p. 947-973, 2005. DOI: <https://doi.org/10.1175/JAS3385.1>.
- REUTERS, A. S. **China see post-lockdowns rise in air pollution: study**. Available: <https://cutt.ly/Nn20>. Access in: 09/14/2020.
- RIVERA, E. A. C. **Systemic Model to Understand the Eutrophication Process in a Water Reservoir**. 2003. Dissertation (Master in Food Engineering) – Faculty of Food Engineering, State University of Campinas, Campinas, 2003. Available: <https://pdfs.semanticscholar.org/13cd/883cf96e0de76fa8f21bdecf52798cc0aa5c.pdf>. Access in: 09/11/2020.
- SEINFELD J.H., PANDIS S.N. **Atmospheric Chemistry and Physics From: Air Pollution to Climate Change** (2nd), John Wiley and Sons (2006). Available: <https://bit.ly/3d2AB50>. Access in: 09/09/2020.
- SILVA, M. P. et al. **Identification of areas of potential eutrophication in the lake of sobradinho-ba using remote sensing**. In: 26th Brazilian Congress of Sanitary and Environmental Engineering, 2011. Available at: <http://abes.locaweb.com.br/XP/XP-EasyArtigos/Site/Uploads/Evento19/Trabalhos CompletosPDF/IV-239.pdf>. Access in: 09/03/2020.
- SOUZA, A.; SANTOS, D. A. S.; CLADIN, L. P. G. Urban air pollution from MODIS aerosol data: effect of meteorological parameters. **Bol. Goia. Geogr.**, v. 37, n. 3, p. 466-483, 2017. Available: <https://www.redalyc.org/pdf/3371/337154296006.pdf>. Access in: 10/22/2020.
- UN - United Nations, 2019. Revision of World Population Prospect. Available at: <https://population.un.org/wpp/>. Access in: 10/18/2020.

AUTHORS' CONTRIBUTION

Laízy de Santana Azevedo conceptualized, designed the methodology, analyzed and wrote it. Ana Lúcia Bezerra Candeias and João Rodrigues Tavares Junior supervised and wrote.



This is an Open Access article distributed under the terms of the Creative Commons Attribution License, which permits unrestricted use, distribution, and reproduction in any medium, provided the original work is properly cited